Graphical Abstract

To create your abstract, type over the instructions in the template box below.
Fonts or abstract dimensions should not be changed or altered.

Probing cytochrome P450 bioactivation and fluorescent properties with morpholinyl-tethered anthraquinones

Leave this area blank for abstract info.

Rachel J. Errington, Maria Sadiq, Laura Cosentino, Marie Wiltshire, Omair Sadiq, Marcella Sini, Enric Lizano, M. Dolors Pujol, Goreti R. Morais, Klaus Pors

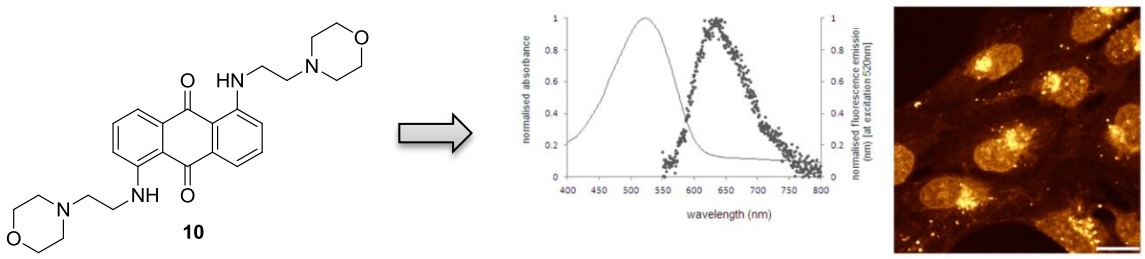

Probing cytochrome P450 bioactivation and fluorescent properties with morpholinyl-tethered anthraquinones

Rachel J. Errington[a,*], Maria Sadiq[b], Laura Cosentino[a,b], Marie Wiltshire[a], Omair Sadiq[b], Marcella Sini[b], Enric Lizano[b,c], M. Dolors Pujol[c], Goreti R. Morais[b], Klaus Pors[b,*]

[a]*Tumour MicroEnvironment Group, Division of Cancer and Genetics, School of Medicine, Cardiff University, Tenovus Building, Cardiff, CF14 4XN, U.K.*
[b]*Institute of Cancer Therapeutics, School of Pharmacy and Medical Sciences, Faculty of Life Sciences, University of Bradford, BD7 1DP, U.K..*
[c]*Laboratori de Química Farmacèutica (Unitat Associada al CSIC). Facultat de Farmàcia. Universitat de Barcelona. gonal 643. E-08028-Barcelona, Spain.*

ARTICLE INFO

Article history:
Received
Revised
Accepted
Available online

Keywords:
Anthraquinone; nemorubicin, MMDX, DRAQ5, cytochrome P450, CYP1A2, fluorophore, cancer

ABSTRACT

Structural features from the anticancer prodrug nemorubicin (MMDX) and the DNA-binding molecule DRAQ5™ were used to prepare anthraquinone-based compounds, which were assessed for their potential to interrogate cytochrome P450 (CYP) functional activity and localisation. 1,4-disubstituted anthraquinone **8** was shown to be 5-fold more potent in EJ138 bladder cancer cells after CYP1A2 bioactivation. In contrast, 1,5-*bis*((2-morpholinoethyl)amino) substituted anthraquinone **10** was not CYP-bioactivated but was shown to be fluorescent and subsequently photo-activated by a light pulse (at a bandwidth 532 to 587 nm), resulting in punctuated foci accumulation in the cytoplasm. It also showed low toxicity in human osteosarcoma cells. These combined properties provide an interesting prospective approach for opto-tagging single or a sub-population of cells and seeking their location without the need for continuous monitoring.

The cytochrome P450 (CYP) enzymes are responsible for the oxidation of a diverse range of xenobiotic and endogenous compounds. There are 57 transcriptionally active genes encoding CYPs, which are classified into families and subfamilies according to their nucleotide sequence.[1] CYPs function mainly to detoxify xenobiotics and endogenous molecules, but some evidence also indicates a link to signaling events.[2] Many probes based on various chemical scaffolds have been explored in order to identify chromophores that can be used to explore CYP activity.[3] Generally, it has proven difficult to develop CYP isoform-selective fluorophores, in particular because CYPs are encoded by large gene families, and their functions cannot be predicted from their gene sequence.[4] However, it is possible to achieve CYP-selectivity as we have shown with duocarmycin bioprecursors reengineered to target CYP1A1 and CYP2W1 for tumour-selective bioactivation.[5-7] However, the duocarmycin scaffold[8] is not suited as a fluorophore for monitoring CYP functional activity as the pharmacophore is poorly fluorescent.

Nemorubicin (3'-deamino-3'-[2-(*S*)-methoxy-4-morpholinyl]doxorubicin; MMDX, **1**), a doxorubicin derivative bearing a methoxymorpholinyl group on the carbohydrate moiety, has undergone clinical evaluation.[9] MMDX is at least 80-fold more potent *in vivo* compared with doxorubicin, which is attributed to generation of metabolite PNU-159682 (**2**) via CYP3A bioactivation that can covalently adduct DNA.[10, 11] The latter is likely to follow DNA intercalation via the planar anthraquinone pharmacophore, which we have explored to discover libraries of dual-targeting DNA-affinic covalent binding agents.[12-18] The anthraquinone also plays a key part in the anticancer drug mitoxantrone (**3**) and DRAQ5 (**4**), a far-red DNA label used to detect nuclei and quantify DNA content in live or fixed cells.[19, 20] The anthraquinone possesses fluorescent properties that can be exploited in measuring nuclear or cytoplasmic events.[21] Here, we speculated whether combining features of MMDX and DRAQ5™ could be used to discover new molecules, which could simultaneously be used to assess CYP functional activity across a heterogeneous cell population.

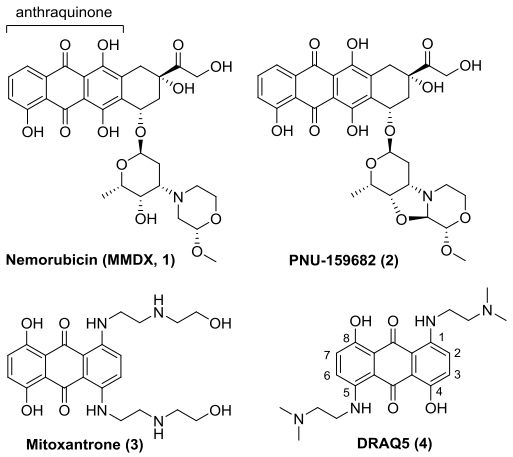

Figure 1 Anthraquinone-based bioactive compounds

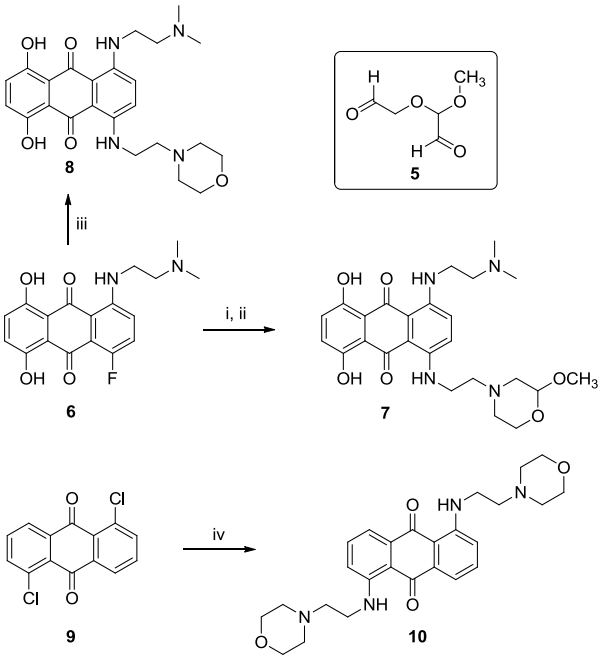

Scheme 1 Synthesis of target compounds 7, 8 and 10. (i) $H_2NCH_2CH_2NH_2$ (neat), 42%, (ii) **5**, $NaBH_3CN$, glacial acetic acid, 32%, (iii) amine (neat), 78%, (iv) excess amine (neat), 50 ºC, 1-3 h, 60-85%

Synthesis of target anthraquinone probes **7**, **8** and **10** were prepared from either 1-monosubstituted building block **6** or commercially available **9**. Compound **6** was reacted with neat ethylenediamine and purified by column chromatography before the resulting 1,4-disubsituted aminoanthraquinone was reacted with 2-methoxy-2-(2-oxoethoxy)acetaldehyde **5** under reductive amination conditions to produce target molecule **7**.[22] Intermediate **5** was generated following the published procedure.[23] Anthraquinone probes **8**[24] and **10**[25, 26] were obtained by stirring **6** or **9** respectively in neat 2-morpholinoethylamine followed by removal of excess amine and purification by flash column chromatography.

To determine if compounds **7** and **8** were substrates for CYP bioactivation. We evaluated these in the EJ138 bladder cancer cell line (identical to the T24 cell line[27]) due to its very low levels of CYPs.[6] Using previously published methodology,[28] metabolites were generated via incubation of compounds **7** and **8** with 20 pmol CYP bactosomes in 50 mM Tris-HCl buffer (2 mM NADPH, 1 mM $MgCl_2$, pH 7.4). Generally, none of the extracted metabolite incubates were shown to exert increased anti-proliferative activity over their parental compounds **7** and **8** using the MTT assay (Table 1). The only exception was that CYP1A2-mediated metabolites from incubation with compound **8** possessed approximately a 5-fold potentiation in activity. Evaluation was also performed in SW480-mock and 2W1-transfected colon carcinoma cell lines,[7] but no bioactivation was observed for compounds **7** (IC_{50} = 1.27 μM in mock cells and 1.53 μM in CYP2W1 cells) and **8** (IC_{50} = 0.97 μM in mock cells and 1.25 μM in CYP2W1 cells).

Both the morpholinyl and 2-methoxymorpholinyl moieties contain motifs that could be hydroxylated by CYPs in the 3-position with loss of H_2O and generation of activated imine or hydroxylation at the 3-methoxy group with loss of formaldehyde, ring opening and generation of an aldehyde intermediate. Such CYP-bioactivated metabolites would have the propensity to form covalent adducts with DNA and hence increased potency would be expected. However, the lack of any significant bioactivation by CYP3A4 and 3A5 indicates that the carbohydrate moiety of **1** in the proximity of the 2-methoxymorpholino group, subsequent to CYP3A hydroxylation, is vital for intramolecular formation of a potent cytotoxin and emphasizes the importance of the MMDX structural configuration.[10]

To investigate the fluorescent properties of the compounds we decided to use human non-small cell lung (A549) and osteosarcoma (U2-OS) cancer cell lines, which we routinely use as models for assessing compounds with fluorescent properties[20, 29]; these cell lines are also relevant for studying CYP1A2 as the human protein atlas shows moderate expression levels of its isoform in both cell types, with U-2 OS cancer cells showing 2-fold RNA levels above A549 cancer cells.[30]

The absorbance spectrum of **7** alone (Fig. 2A) gave two maxima at wavelengths 610 and 650 nm; with an emission profile peak at 690nm and hence the compound can be best detected at a bandwidth of 650-790 nm. The molecule was readily taken up by living A549 cells and was shown to be localised in the peri-nuclear vesicular region of cells (Fig. 2D). The lack of DNA binding by compound **7** is evidenced by a nuclear-to-cytoplasmic (n/c) ratio of fluorescence intensity of 0.3± 0.06 (n= 9). In contrast, the benchmark molecule DRAQ5™ gave a similar far-red spectral performance, but a n/c ratio of 7.7 ±1.8 (n=6). Unlike compounds **7** and **10** DRAQ5™ has two highly DNA affinic moieties in the 1,5 position of the anthraquinone chromophore, giving an equilibrium of nuclear compartment localisation and hence the molecule binds DNA in a stoichiometric fashion. Next we interrogated molecule **10** without the 3-methoxy functionality to assess the effect of the unsubstituted morpholinyl moiety on fluorescent signal while maintaining the 1,5-disubstituted anthraquinone symmetry. This probe showed a blue-shifted absorbance profile to a single peak of 520nm with an emission profile maxima at 635nm (Fig. 2B). However, continuous exposure to 20μM of **10** again in A549 cells resulted in a distinct nuclear labelling and a perinuclear compartment which also contained bright punctate labelling (Fig 2E) and a n/c ratio of 4.1 ± 0.7 (n=17). The lower ratio compared to DRAQ5™ indicated that this molecule can be found in both these compartments. In addition the bright punctate labelling was acquired as a result of the pulsed light exposure (Fig 2E). Compounds **7** and **10** were then loaded into cells within a context of a timelapse screen to determine if the monitored cells were able to continue to undergo cell proliferation when exposed to 2 or 20μM. U-2 OS cells exposed to the high dose of compound **10** continued to proliferate after 48 hours (Fig. 3A) compared to **7** where there was evidence of cell death at this dose (not shown).

Recently, we reported on compound **10** and its ability to stabilise i-Motif forming DNA sequences and found it a poor ligand in contrast to mitoxantrone and other anthraquinones.[25] Interestingly, in this study, **10** was activated by light (at a bandwidth 532 to 587 nm), resulting in punctuated foci accumulation in the cytoplasm (not the nucleus), probably this is

Table 1. Growth inhibition of parental anthraquinone and CYP bactosomes generated metabolite fractions against EJ138 cell line

ID	EJ138	CYP1A1	PF	CYP1A2	PF	CYP1B1	PF	CYP2D6	PF	CYP3A4	PF	CYP3A5	PF
7	0.32 ± 0.02	0.28 ± 0.06	1.1	0.25 ± 0.04	1.3	0.34 ± 0.04	0.9	0.31 ± 0.05	1.0	0.29 ± 0.09	1.1	0.25 ± 0.02	1.3
8	0.34 ± 0.04	0.30 ± 0.08	1.1	0.07 ± 0.01	4.6	0.28 ± 0.09	1.2	0.25 ± 0.06	1.3	0.33 ± 0.06	1.0	0.36 ± 0.02	0.9

[a] IC_{50} (μM) values are the mean ± SD of at least three independent assays; PF = potentiation factor

due to the morpholino ring and independent of the 2-methoxymorpholino functionality (Fig 3B). To our knowledge there is no report of such observation in the literature and thus warrants further investigation.

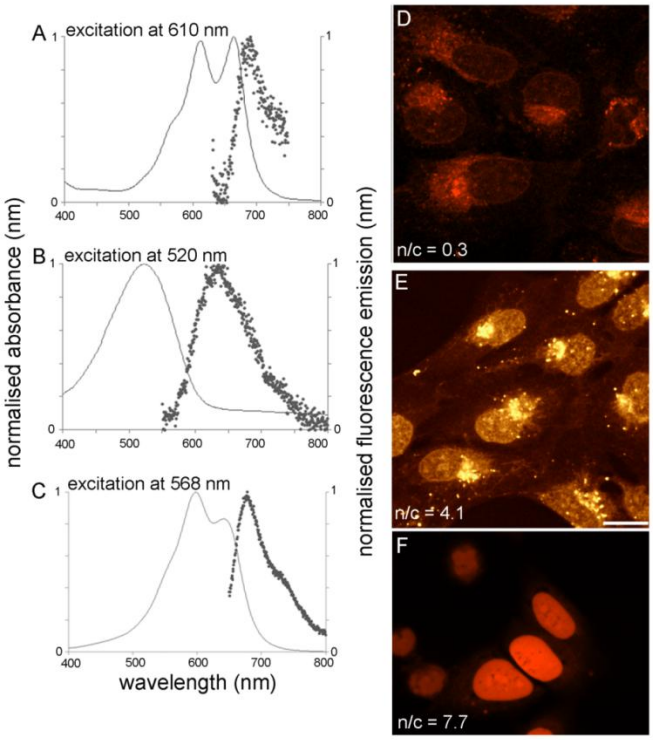

Figure 2. **Fluorescence profiles and cellular localisation of 7 and 10 benchmarked against DRAQ5™**. Absorbance spectrum (line) and associated fluorescent emission spectrum, as a result of excitation at 610nm (dots) for compound **7** (A) and 520nm for **10** (B) and DRAQ5™ (C). Single optical section of A549 cells obtained using confocal laser scanning microscopy. Images captured after 1h (20 µM) exposure of **7** (D) and **10** (E) and DRAQ5™ (F). Note also the nuclear to cytoplasmic ratio of mean fluorescence in each compartment is also given. Bar = 10µm

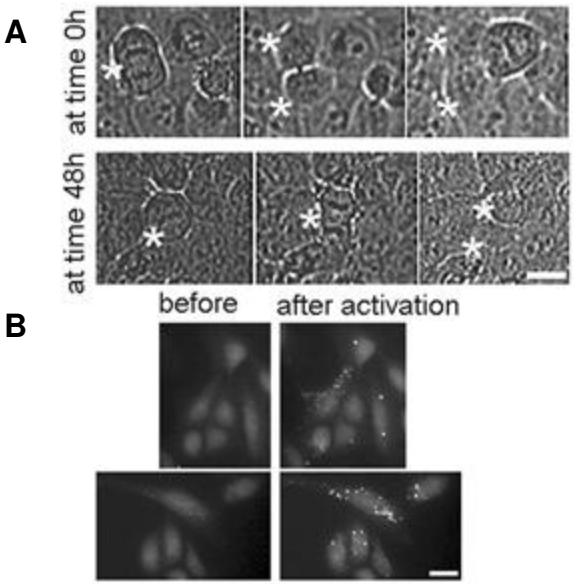

Figure 3. **Compound 10 shows low toxicity and photo-activation properties at 20µM in human osteosarcoma cells (U-2 OS) over 48 hours**. (A) Short phase contrast timelapse sequence (each 20 mins apart) showed cell division was prevalent at time 0h and after a 48 hour exposure in live U-2 OS cells; *indicates the location of mitosis and the subsequent two daughter cells. (B) Fixed U-2 OS cells labelled with **10** for 1 hr, exposed to a 250ms pulse of excitation light (using a x20 0.8NA lens), excitation 560/40nm and emission detection at 630/75 nm. A second identical exposure caused the appearance of punctate foci located in the cytoplasm. This was not to the same extent across all cells. Bar = 10 µm

The 2-methoxymorpholinyl moiety tethered to the anthraquinone did not result in CYP3A bioactivation as previously demonstrated for MMDX, however the simpler morpholinyl analogue **8** was 5-fold bioactivated by CYP1A2 bactosomes. Further medicinal chemistry optimisation of **8** could lead to a probe, which could be used to track CYP1A2 functional activity in human cells. Furthermore, the 1,5-disubstituted scaffold as in probe **10** is a useful starting point for more focused structure-activity relationship studies aimed at determining selective probes with punctuated fluorescent emission/excitation signature together with limited background sample auto-fluorescence. These unique properties provide the capacity for specific cell opto-tagging (through a directed laser beam or aperture illumination), where these cells, with the acquired activated punctate features, can be identified at a subsequent time point without the need for continuous observation - hence a potential tool for monitoring selective cell fate.

References and Notes

1. Patterson LH, Murray GI. *Curr Pharm Des.* 2002;8(15): 1335-1347.
2. Rodriguez-Antona C, Ingelman-Sundberg M. *Oncogene.* 2006;25(11): 1679-1691.
3. Bruno RD, Njar VC. *Bioorg Med Chem.* 2007;15(15): 5047-5060.
4. Sellars JD, Skipsey M, Sadr Ul S, et al. *ChemMedChem.* 2016;11(11): 1122-1128.
5. Pors K, Loadman PM, Shnyder SD, et al. *Chem Commun (Camb).* 2011;47(44): 12062-12064.
6. Sutherland M, Gill JH, Loadman PM, et al. *Mol Cancer Ther.* 2013;12(1): 27-37.
7. Travica S, Pors K, Loadman PM, et al. *Clin Cancer Res.* 2013.
8. Ghosh N, Sheldrake HM, Searcey M, Pors K. *Curr Top Med Chem.* 2009;9(16): 1494-1524.
9. Danesi R, Agen C, Grandi M, Nardini V, Bevilacqua G, Del Tacca M. *Eur J Cancer.* 1993;29A(11): 1560-1565.
10. Quintieri L, Geroni C, Fantin M, et al. *Clin Cancer Res.* 2005;11(4): 1608-1617.
11. Ripamonti M, Pezzoni G, Pesenti E, et al. *Br J Cancer.* 1992;65(5): 703-707.
12. Pors K, Paniwnyk Z, Teesdale-Spittle P, et al. *Mol Cancer Ther.* 2003;2(7): 607-610.
13. Pors K, Paniwnyk Z, Ruparelia KC, et al. *J Med Chem.* 2004;47(7): 1856-1859.
14. Casely-Hayford MA, Pors K, James CH, Patterson LH, Hartley JA, Searcey M. *Org Biomol Chem.* 2005;3(19): 3585-3589.
15. Pors K, Plumb JA, Brown R, et al. *J Med Chem.* 2005;48(21): 6690-6695.
16. Pors K, Shnyder SD, Teesdale-Spittle PH, et al. *J Med Chem.* 2006;49(24): 7013-7023.
17. Abdallah QM, Phillips RM, Johansson F, et al. *Biochem Pharmacol.* 2012;83(11): 1514-1522.
18. Thomas A, Perry T, Berhane S, et al. *Oncogene.* 2015;34(25): 3336-3348.
19. Smith PJ, Wiltshire M, Errington RJ. *Curr Protoc Cytom.* 2004;Chapter 7: Unit 7 25.
20. Njoh KL, Patterson LH, Zloh M, et al. *Cytometry A.* 2006;69(8): 805-814.
21. Edward R. *Mol Cells.* 2009;27(4): 391-396.
22. 1-((2-(dimethylamino)ethyl)amino)-5,8-dihydroxy-4-((2-(2-methoxymorpholino)ethyl)amino)anthracene-9,10-dione (Compound 7).

1H NMR (400 MHz, CDCl3): δ (ppm) 13.45 (s, 2H), 10.45 (broad s, 2H), 7.1 (m, 2H), 7.05 (s, 2H), 4.61 (s, 1H), 3.93 (t, 1H), 3.55 (m, 1H), 3.49 (m, 3H), 3.47 (d, 1H), 3.4 (s, 3H), 3.33 (t, 2H), 2.7 (t, 2H),

2.43 (m, 4H), 2.35 (s, 6H); 13C NMR (101 MHz, CDCl3): δ (ppm) 185.88; 153.14, 146.01, 125.15, 123.34, 122.73, 115.11,112.88, 109.23, 57.19, 56.10, 54.36, 53.12, 45.83, 41.04, 42.31, 26.13, 25.43.); m/z 485 ([M+H]+, 100%); HRMS (m/z): [M + H]+ calcd for C25H32N4O6, 484.2322; found, 484.2375.
23. Bargiotti A, Grandi M, Suarato A, Faiaridi D. *United States Patent.* 1994;Patent Number: US005304687A.
24. 1-((2-(dimethylamino)ethyl)amino)-5,8-dihydroxy-4-((2-morpholinoethyl)amino)anthracene-9,10-dione (Compound 8)
1H NMR (400 MHz, CDCl3): δ (ppm) 13.48 (s, 2H), 10.52 (broad s, 2H), 7.15 (m, 2H), 7.12 (s, 2H), 3.65 (m, 6H), 3.45 (m, 4H), 2.7 (t, 2H), 2.43 (m, 4H), 2.35 (s, 6H); 13C NMR (101 MHz, CDCl3): δ (ppm) 185.59; 153.34, 145.71, 124.85, 123.94, 122.34, 115.15, 111.28, 57.13, 53.36, 53.66, 45.63, 41.62, 42.44, 26.33, 25.89; m/z 455 ([M+H]+, 100%); HRMS (m/z): [M + H]+ calcd for C25H32N4O6, 454.2216; found, 454.2251.
25. Wright EP, Day HA, Ibrahim AM, et al. *Sci Rep.* 2016;6: 39456.
26. Katzhendler J, Gean KF, Barad G, et al. *European Journal of Medicinal Chemistry.* 1989;24(1): 23-30.
27. O'Toole CM, Povey S, Hepburn P, Franks LM. *Nature.* 1983;301(5899): 429-430.
28. Vinader V, Sadiq M, Sutherland M, et al. *Medchemcomm.* 2015;6(1): 187-191.
29. Smith PJ, Wiltshire M, Chappell SC, et al. *Cytometry A.* 2013;83(1): 161-169.
30. The Human Protein Atlas: https://www.proteinatlas.org/ENSG00000140505-CYP1A2/cell; Accessed 7 March 2018.